RESEARCH ARTICLE

Targeting foam cell formation in inflammatory brain diseases by the histone modifier MS-275

Bettina Zierfuss[1] [iD], Isabelle Weinhofer[1] [iD], Agnieszka Buda[1] [iD], Niko Popitsch[2], Lena Hess[3], Verena Moos[3], Simon Hametner[4], Stephan Kemp[5], Wolfgang Köhler[6], Sonja Forss-Petter[1], Christian Seiser[3] & Johannes Berger[1] [iD]

[1]Department of Pathobiology of the Nervous System, Centre for Brain Research, Medical University of Vienna, Vienna, 1090, Austria
[2]Institute of Molecular Biotechnology, Vienna, 1030, Austria
[3]Division of Cell and Developmental Biology, Center for Anatomy and Cell Biology, Medical University of Vienna, Vienna, 1090, Austria
[4]Department of Neuropathology and Neurochemistry, Medical University of Vienna, Vienna, 1090, Austria
[5]Laboratory Genetic Metabolic Diseases, Amsterdam UMC, Amsterdam Gastroenterology & Metabolism, Amsterdam Neuroscience, University of Amsterdam, Amsterdam, 1105AZ, The Netherlands
[6]Department of Neurology, University of Leipzig Medical Centre, Leukodystrophy Clinic, Leipzig, 04103, Germany

Correspondence
Johannes Berger, Department of Pathobiology of the Nervous System, Spitalgasse 4, 1090 Vienna, Austria. Tel: +43-1-40160 34300; Fax: +43-1-40160 934203; E-mail: johannes.berger@meduniwien.ac.at

Abstract

Objective: To assess class I-histone deacetylase (HDAC) inhibition on formation of lipid-accumulating, disease-promoting phagocytes upon myelin load in vitro, relevant for neuroinflammatory disorders like multiple sclerosis (MS) and cerebral X-linked adrenoleukodystrophy (X-ALD). **Methods**: Immunohistochemistry on *postmortem* brain tissue of acute MS ($n = 6$) and cerebral ALD ($n = 4$) cases to analyze activation and foam cell state of phagocytes. RNA-Seq of in vitro differentiated healthy macrophages ($n = 8$) after sustained myelin-loading to assess the metabolic shift associated with foam cell formation. RNA-Seq analysis of genes linked to lipid degradation and export in MS-275-treated human HAP1 cells and RT-qPCR analysis of HAP1 cells knocked out for individual members of class I HDACs or the corresponding enzymatically inactive knock-in mutants. Investigation of intracellular lipid/myelin content after MS-275 treatment of myelin-laden human foam cells. Analysis of disease characteristic very long-chain fatty acid (VLCFA) metabolism and inflammatory state in MS-275-treated X-ALD macrophages. **Results**: Enlarged foam cells coincided with a pro-inflammatory, lesion-promoting phenotype in *postmortem* tissue of MS and cerebral ALD patients. Healthy in vitro myelin laden foam cells upregulated genes linked to LXRα/PPARγ pathways and mimicked a program associated with tissue repair. Treating these cells with MS-275, amplified this gene transcription program and significantly reduced lipid and cholesterol accumulation and, thus, foam cell formation. In macrophages derived from X-ALD patients, MS-275 improved the disease-associated alterations of VLCFA metabolism and reduced the pro-inflammatory status of these cells. **Interpretation**: These findings identify class I-HDAC inhibition as a potential novel strategy to prevent disease promoting foam cell formation in CNS inflammation.

Introduction

In neuroinflammation, CNS-resident microglia and infiltrating macrophages are crucial for the clearance of lipid-rich myelin to promote remyelination.[1–4] Upon myelin phagocytosis, these cells adopt an enlarged foamy morphology similar to lipid-laden macrophages in atherosclerotic plaques.[1,5–7] In the inflammatory demyelinating disease multiple sclerosis (MS), foam cells in CNS lesions undergo a tri-phasic pattern of polarization.[6] In the first phase, the uptake of myelin leads to a disease-promoting phenotype associated with secretion of pro-inflammatory cytokines and toxic mediators. In a second phase, intracellular lipid mediators produced by myelin

digestion induce an anti-inflammatory program, probably through activation of the nuclear receptors liver X receptor (LXR) and peroxisome proliferator-activated receptor (PPAR). This change in gene transcription patterns enables phagocytes to export excess lipids, while secretion of anti-inflammatory cytokines facilitates remyelination. In the pathological context of MS, foam cells are challenged with export of accumulated cholesterol-rich myelin debris. Thus, a third phase is triggered, which is characterized by foam cells with lipid inclusions favoring a lasting disease-promoting phenotype.[6] Myelin-laden foam cells are also present in brain lesions of patients with the neuroinflammatory demyelinating disease X-linked adrenoleukodystrophy (X-ALD).[8] X-ALD is caused by mutations in the *ATP-binding cassette subfamily D member 1 (ABCD1)* gene, which results in impaired very long-chain fatty acid (VLCFA) metabolism.[9–11] Accordingly, X-ALD patients show characteristic VLCFA accumulation in tissues and body fluids, particularly in cell types with high cholesterol turnover.[9,12] About 60% of male X-ALD patients develop cerebral ALD (CALD), a rapidly progressive inflammatory demyelination of the brain.[13–15] When applied at an early disease stage, hematopoietic stem cell transplantation or gene therapy can rescue CALD patients from major disabilities.[16–18] The underlying mechanism might be the exchange of mononuclear phagocytes, which are the immune cells most severely affected by the disturbed VLCFA metabolism.[19] Therefore, metabolic reprogramming of these cells could be a novel approach to interfere with the neuroinflammation in CALD patients.[8,19] We recently demonstrated that application of the pan-histone deacetylase (HDAC) inhibitor Vorinostat (SAHA) partially rescued immunological and metabolic defects in X-ALD macrophages.[20] A particular member of the class I HDAC family, HDAC3, was found to be crucial for regulating lipid metabolism in murine macrophages,[21–23] with deletion of *Hdac3* leading to significantly reduced lipid accumulation and foam cell numbers in a murine atherosclerosis model.[21] This was possibly mediated by increased expression of genes in pathways associated with LXRα and PPARγ.[21] Here, we hypothesize that the selective inhibition of class I HDACs using the pharmacological compound MS-275 (Entinostat) may improve the lipid/cholesterol homeostasis in human lipid-laden phagocytes upon sustained myelin debris accumulation in demyelinating disorders like CALD. Therefore, we investigated the role of HDAC1-3 in lipid metabolism of primary human monocyte-derived macrophages and assessed the efficacy of MS-275 to prevent foam cell formation in vitro. Furthermore, we tested whether MS-275 could correct the disease-associated alterations in macrophages derived from X-ALD patients.

Subjects/Materials and Methods

Patients and healthy volunteers

Peripheral blood samples were drawn from 35 healthy volunteers (age 24–61 years, median = 37 years) and from four X-ALD patients with the default disease variant adrenomyeloneuropathy (AMN; age 25–44 years, median = 38 years, Table S1). At the time of blood donation, none of the AMN patients revealed any signs of cerebral involvement on MRI. VLCFA accumulation in plasma and leukocytes of AMN patients was confirmed by measuring the total amount of the fatty acids C26:0, C24:0, and C22:0 by GC-MS or in macrophages by LC-MS/MS as described previously.[19,24] The in vitro study of human primary macrophages was approved by the Ethical Committee of the Medical University of Vienna (EK1462/2014), and informed consent was obtained from participating AMN patients and healthy volunteers. Histochemistry was performed using *post-mortem* CNS tissue. Details of the patients' characteristics and conditions have been summarized previously.[8] Use of this material was approved by EK729/2010 and EK535/2016.

Isolation of human monocytes

Human CD14^{+} monocytes were isolated from blood by magnetic-activated cell sorting as described previously.[19]

Flow cytometry

The purity of isolated CD14^{+} monocytes was determined by flow cytometry as described previously.[8] To analyze the number of pHrodo Green-positive macrophages, the cells were detached, washed and re-suspended in 250 μL phosphate-buffered saline (PBS) before analysis. Viable macrophages were gated using forward and side scatter. Geometric mean of fluorescence intensity (gMFI) was determined from 5000 macrophages per sample and using a GuavaEasyCyte™6-2L system flow cytometer (Luminex) and guavaSoft3.3 software.

In vitro differentiation of human monocytes to macrophages and activation with lipopolysaccharide (LPS)

CD14^{+} monocytes (1×10^6 cells/well) were cultured in RPMI medium (Sigma Aldrich) containing 1% Penicillin/Streptomycin, 1% glutamine, 1% Fungizone and 10% FCS, supplemented with 50 ng/mL human recombinant M-CSF (PeproTech) for 7 days. For use in β-oxidation assays, M-CSF-differentiated macrophages were

polarized with 100 ng/mL IL-4 (Novartis) for 2 days in the presence of 10 ng/mL M-CSF. The HDAC inhibitors SAHA (Cat.No.10009929, Cayman Chemicals) and MS-275 (Cat.No.T6233, Target Mol) were added during the last 48 h. For analysis of pro-inflammatory cytokine gene expression, M-CSF-differentiated macrophages were stimulated with 100 ng/mL LPS (*E. coli* 055:B5, Cat.no. L4005, Sigma) and treated with DMSO, MS-275, or SAHA in concentrations as indicated for 24 h. For detachment, adherent macrophages were washed with PBS and incubated with 300 μL Gibco™TrypLE™Select (10×) (Gibco, Life Technologies) for 15 min at 37°C, and collected with a cell scraper after adding 300 μL PBS.

Generation of foam cells and determination of neutral lipids and total cholesterol

Human blood-derived monocytes were differentiated using 50 ng/mL M-CSF in the presence of 20 μg/mL myelin for 7 days during differentiation to generate myelin-laden foam cells and the viability was determined by flow cytometry using the fluorescent dye 7-AAD detecting dead cells (Fig. S3).

Then, foam cells were incubated with DMSO or MS-275 as indicated for 24 h before harvesting for RNA analysis of gene expression or 48 h for assays of neutral lipids and total cholesterol content. The myelin was isolated from wild-type C57BL6/J mouse brains and the purity was determined by western blotting with specific antibodies as described and shown in detail previously.[8] Endotoxin levels were determined by Genscript ToxinSensorTM Chromogenic LAL Endotoxin Assay Kit and were far below the threshold (<0.5 EU/mL) for medicinal products. Part of the myelin was labeled with the amine-reactive pH-sensitive dye pHrodo®GreenSTP ester (Thermo Fisher Scientific, Cat.No.:P35369) according to the manufacturer's instructions as described previously.[8]

Neutral lipids were visualized in the cultured cells after fixation in 4% paraformaldehyde by Oil Red-O (C.I. 26125, Merck, Certistain®, ORO) staining. For analysis of cellular cholesterol content, the harvested cells were washed with PBS before lipid extraction by sonication on ice in chloroform-methanol (v/v 2:1). After centrifugation, the organic phase was transferred to a fresh tube and air dried at 50°C. The dried lipids/ cholesterol were re-dissolved in reaction buffer (Component E) of the Amplex Red Cholesterol Assay Kit (Molecular Probes, Invitrogen/Thermo Fisher) and total cholesterol was measured according to the manufacturer's instructions.

Immunohistochemical staining of macrophages/microglial cells in active demyelinating lesions of *postmortem* CNS tissue

Paraffin-embedded *postmortem* tissue containing active demyelinating brain lesions was available from four CALD cases and six MS cases as described previously[8] and further outlined in Table S2. Immunohistochemical staining for the pro-inflammatory macrophage/microglia marker CD86 was performed as described before.[8] To determine the size (cross-sectional area in μm^2) of macrophages/microglia in active demyelinating lesions sections were steamed in citrate buffer (pH 6.0) for 1 h and stained using the primary rabbit antibodies against p22-phox (Santa Cruz #sc20781) diluted 1:100 in 10% FCS/ Dako buffer and applied over night at 4°C. A secondary biotinylated anti-rabbit antibody (Jackson#711-065-152, diluted 1:1000) was applied, followed by avidin-conjugated horse-radish peroxidase (Jackson#016-030-084, diluted 1:500) for 1 h, both at room temperature. Sections were developed with 3,3′-diaminobenzidine and counterstained with hematoxylin. To quantify the cross-sectional area of p22phox positive macrophages/microglia, the software Image J was used. In addition, histochemical myelin staining was performed using a routine Luxol fast blue-periodic acid Schiff (LFB-PAS) protocol,[25] visualizing myelin-derived phospholipids and digested glycolipids.

HAP 1 cells

HAP1 cells and *HDAC1, 2 or 3* knockout (KO) HAP1 cell lines were obtained from Horizon Genomics (now, Horizon Discovery). Mutant HAP1 cells expressing FLAG-tagged catalytically inactive enzymes: HDAC1 H141A, HDAC2 H142A, and HDAC3 H135A were generated by CRISPR-Cas9-mediated knock-in of the expression construct under the control of the *EF1a* promoter into the safe harbor locus AAVS1 of the corresponding KO cell lines (V. Moos et al., manuscript in preparation).

Whole transcriptome analysis

Whole transcriptome analysis of human in vitro-generated foam cells was performed for eight healthy volunteers, and differential expression was compared between vehicle-treated and myelin-laden macrophages. Total RNA (100 ng) was used for the generation of mRNA-focused libraries. The samples were sequenced on a HiSeq2000 sequencing system (Illumina) at the Biomedical Sequencing facility of the Medical University of

Vienna, Austria as described previously.[8] After a global analysis of deregulated genes, a targeted analysis of (1) genes from cholesterol, LXR or PPAR pathways as retrieved from the Molecular Signatures Database (MSigDB) and (2) cytokine-cytokine receptor interaction pathway genes (KEGG pathways:map04060) for pro- and anti-inflammatory gene expression was performed (Dataset S1).

Whole transcriptome analysis of HAP1 cells was performed for three biological replicates each after treatment with 1 μmol/L or 3 μmol/L MS-275 for 24 h, samples were compared to vehicle (DMSO)-treated cells ($n = 3$). Here, we considered, only significantly changed genes (in comparison to vehicle controls) from the cholesterol, LXR or PPAR pathways, as described for foam cells. The complete dataset from these pathways is shown in Dataset S2.

RNA isolation and reverse transcription-coupled quantitative PCR (RT-qPCR)

RNA isolation and RT-qPCR analysis were carried out as previously described.[8,19] Each cDNA was measured in technical duplicates. Relative mRNA levels were detected by SYBRGreen incorporation and calculated by the $2^{-\Delta\Delta Cq}$ method using *HPRT1* as internal reference. In addition, the absolute mRNA abundance of *ABCD1*, *ABCD2* and for normalization, *HPRT1* were obtained by the TaqMan ^{TM} method. Sequences of primers are shown in Table S3.

Statistical analysis

For normally distributed data, we performed either two-tailed Student's *t*-test or, when more than two groups were analyzed, one-way ANOVA and *post hoc* Fisher's LSD test as indicated. The *P*-values were calculated and the null hypothesis denied for *P*-values < 0.05. The software GraphPad Prism 7 (GraphPad Software) was used for graphical display and statistical analysis.

Further detailed methods are described in the supplementary materials.

Results

Enlarged foam cells in actively demyelinating CNS lesions are associated with inflammation

To assess foam cell formation in acute MS and CALD lesions, we first measured the size of enlarged macrophages/microglia in actively demyelinating lesions of *post-mortem* brain tissue from patients using the lipid-staining LFB-PAS (Fig. 1A and B) and the immunohistochemical

staining for the plasma membrane-accentuated p22phox (Fig. 1C and D). We observed comparable enlarged LFB-PAS positive phagocytes in CALD and MS and obtained similar results when assessing enlarged p22phox-positive foam cells (Fig. 1E–G). Because the smallest sizes in our data unlikely reflect the true cell size, which also depends on the plane at which the cell was cut, merely the highest 75% of the values were included in violin plots of the cell size distribution (Fig. 1E and F). In both diseases, especially enlarged foam cell sizes (3rd quartile of the cell size) coincided with a high number of CD86-positive, pro-inflammatory macrophages/microglia (Fig. 1H–J, Fig. S2), and the presence of a phagocytic, inflammation-associated phenotype evidenced by the marker CD68 (Fig. 1K–M, Fig. S2). Together, these results show that profound myelin debris uptake by macrophages and microglial cells leads to formation of enlarged foam cells in actively demyelinating CNS lesions of both MS and CALD. In addition, especially enlarged foam cells appear to coincide with a pro-inflammatory, disease-promoting environment.

Genome-wide analysis of human myelin-laden macrophages

In contrast to previous studies,[5,26–30] we particularly aimed to investigate the effect of a prolonged myelin accumulation on human macrophages, and thus, performed a genome-wide transcriptome analysis of in vitro-differentiated macrophages, which were derived from healthy donors ($n = 8$) and exposed for 7 days to myelin debris (Fig. 2).

We found that myelin phagocytosis especially downregulated genes involved in cholesterol and fatty acid synthesis, whereas genes involved in intracellular lipid shuttle and export were increased (Fig. 2A). Specifically, myelin-loading prominently induced *NR1H3* and *PPARG* encoding the nuclear receptors LXRα and PPARγ, respectively (Fig. 2A). Whereas some pro-inflammatory genes were significantly downregulated upon myelin ingestion, the expression of genes encoding growth and neurotrophic factors or cytokines and their cognate receptors involved in homeostatic functions was significantly upregulated in myelin-laden macrophages (Fig. 2B). Using RT-qPCR and an enlarged sample set ($n = 13$), we confirmed the differential expression patterns of selected key genes in lipid homeostasis. Furthermore, we analyzed the expression of the characteristic anti-inflammatory genes *CCL18* and *CD83*, which were significantly upregulated after myelin phagocytosis (Fig. 2C–H). Together, these findings indicate that sustained myelin loading of human healthy macrophages in a non-inflammatory environment induce gene expression programs possibly enabling not only efficient lipid degradation and efflux, but also tissue regeneration.
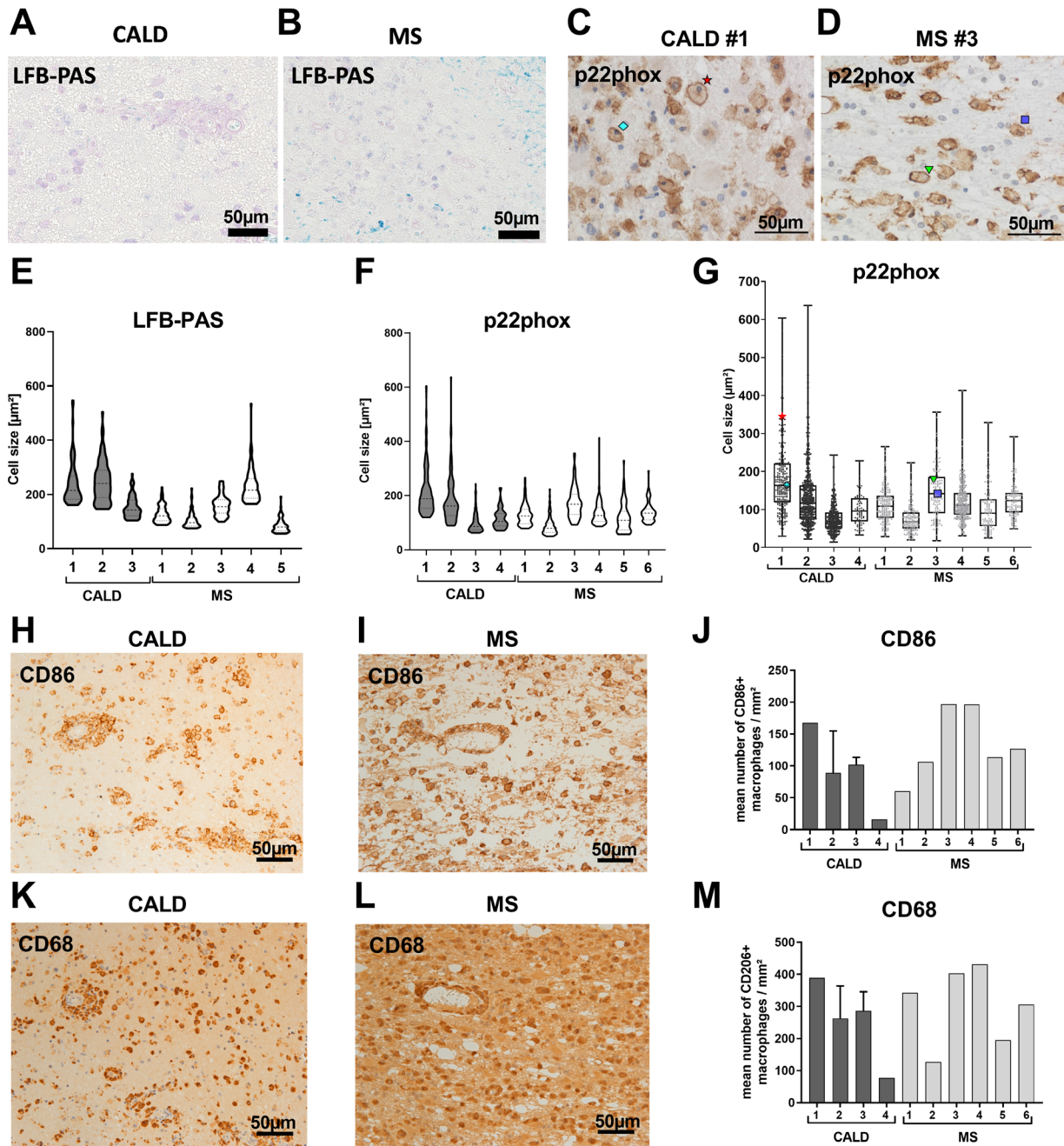
Figure 1. Enlarged foam cells coincide with an increased number of activated and pro-inflammatory macrophages/microglial cells in active demyelinating lesions of the CNS. (A–M): To analyze foam cells, active demyelinating lesions of *postmortem* CNS tissues derived from four cerebral ALD (CALD) and six acute multiple sclerosis (MS) patients were immunohistochemically stained and exemplary images are shown for the lipid staining LFB-PAS (A and B) to detect intact myelin or myelin debris and degraded intermediates of myelin engulfed by foam cells and analyzed for the membrane-accentuated marker p22phox (C and D), the pro-inflammatory marker CD86 (H and I) and the activation and phagocytosis marker CD68 (K and L). Representative images of the p22phox-stained brain lesion edge are shown from CALD case #1 (C) and MS case #3 (D). The cross-sectional area (μm^2) of LFB-PAS (E) or p22phox (F and G) positive macrophage/microglial cells within the active demyelinating lesions is plotted. Symbols in (C and D) indicate the cells/data points of two exemplary cells from CALD #1 (star, diamond) and MS #3 (triangle, square) in (G). The 75% highest values for each data set are described using violin plots in (E and F). The density of pro-inflammatory CD86- and CD68-positive macrophages/microglial cells was determined within the lesion center for each case (J and M). When more than one CNS-region revealing an active demyelinating lesion per case was available, the mean value was determined (CALD #2, $n = 3$ and CALD #3, $n = 2$). Error bars indicate the maximum and minimum in (G) and standard deviation in (J and M). Scale bar = 50 μm.
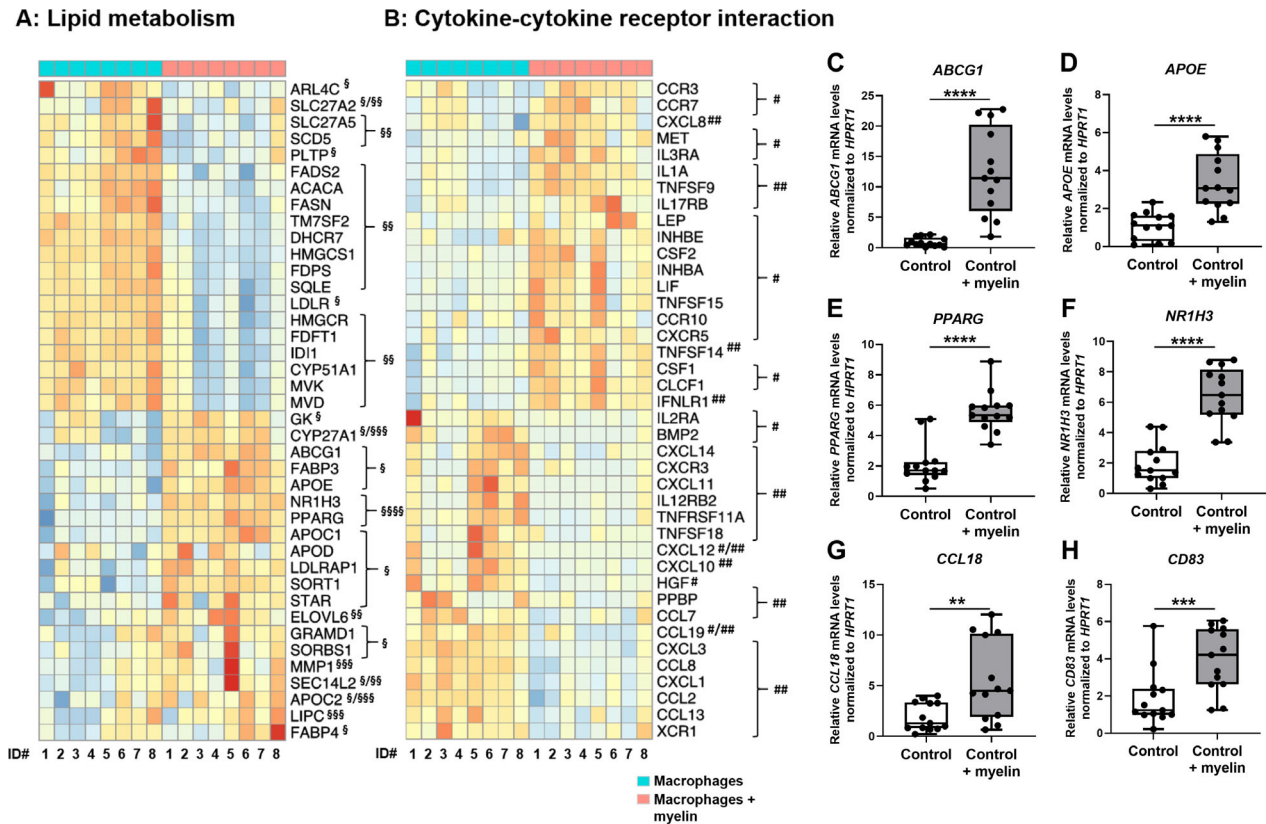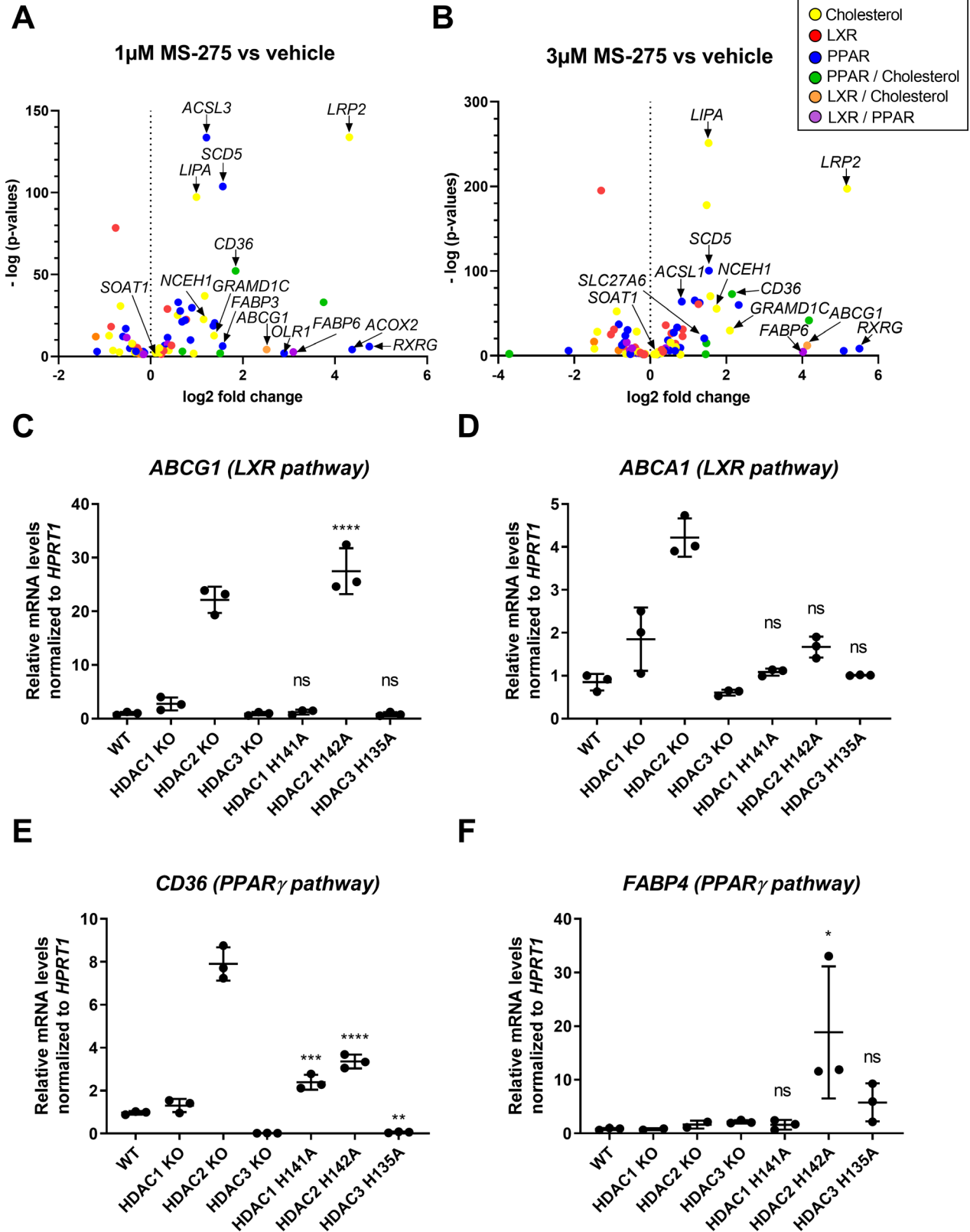
Figure 2. Human foam cells generated in vitro upregulate expression of lipid transport and efflux genes and are associated with a program promoting tissue regeneration. (A and B) Heat maps of normalized expression values for macrophages differentiated in the absence (Macrophages) or the presence (Macrophages + myelin) of myelin. Heatmaps were calculated from variance-stabilized (vst transformed) expression values that were scaled per gene (Z-score) for 20 up- and 20 downregulated genes with maximum absolute log2 fold change from the list of: genes involved in lipid metabolism (A) and genes annotated in the KEGG cytokine/cytokine receptor interaction pathway (B). Genes on the y-axis were sorted by row-mean of the first shown condition. Sample identification numbers (ID#) refer to healthy controls 1-8. (C–H) Confirmation of RNA-Seq results of selected genes involved in lipid metabolism (C–F) or cytokine-cytokine receptor interaction (G and H) pathways by RT-qPCR in a larger sample set of healthy volunteers ($n = 13$). Relative gene expression levels were normalized to the reference gene *HPRT1*. For statistical analysis two-tailed paired Student's *t* test was used. Gene assignments according to their function are indicated by superscript symbols: § transport (uptake, intracellular shuttle and efflux), §§ anabolism, §§§ catabolism, §§§§ nuclear receptors, # homeostasis, ## inflammation. ** $P < 0.01$, ***$P < 0.001$, ****$P < 0.0001$.

Class I HDACs regulate lipid metabolism-associated genes in human macrophages

Next, we tested whether the specific inhibition of class I HDACs, which was previously shown to regulate the lipid metabolism in an atherosclerotic mouse model,[21] could be beneficial to prevent foam cell formation in human macrophages. As an initial screening tool, we used the human cell line HAP1, modified for production of isogenic variants carrying mutations in selected genes.[31] First

Figure 3. Class I HDACs regulate lipid metabolism-associated genes in the human HAP1 cell line. (A and B) The expression levels of lipid metabolism-associated genes were extracted from whole transcriptome RNA-Seq data acquired from the human haploid leukemia cell line HAP1 treated with 1 μmol/L (A) or 3 μmol/L MS-275 (B) for 24 h and compared to vehicle controls ($n = 3$ for each condition). Volcano plots indicate the mean values of log2 fold changes and $-$log transformed *P*-values for each significantly changed gene. (C–F) The contribution of the individual histone deacetylases inhibited by MS-275 to the regulation of key genes in lipid homeostasis was analyzed in mutant HAP1 cells with full knockout (KO) of *HDAC1, 2* or *3* (HDAC1-3 KO) or the same lines with knock-in mutations generating stable but enzymatically inactive HDAC1-3 proteins (HDAC1 H141A, HDAC2 H142A or HDAC3 H135A) ($n = 3$ each). The relative mRNA levels of the LXR-regulated genes *ABCA1* and *ABCG1* (C and D) and the PPARγ-regulated genes *CD36* and *FABP4* (E and F) were analyzed by RT-qPCR and normalized to *HPRT1*. The mean for each group is depicted and error bars indicate standard deviation. For statistical analysis, one-way ANOVA and Fisher's LSD test were used to compare gene expression levels between wild type (WT) samples and the enzymatically inactive variants of HDAC1-3 (HDAC1 H141A, HDAC2 H142A or HDAC3 H135A). ns = not significant, *$P < 0.05$, **$P < 0.01$, ***$P < 0.001$, ****$P < 0.0001$.

A 1μM MS-275 vs vehicle

B 3μM MS-275 vs vehicle

C *ABCG1 (LXR pathway)*

D *ABCA1 (LXR pathway)*

E *CD36 (PPARγ pathway)*

F *FABP4 (PPARγ pathway)*

parental HAP1 cells that had been treated with 1 or 3 μmol/L MS-275 for 24 h were compared to vehicle control in a whole transcriptome analysis. We queried these gene sets selectively for pathways associated with lipid metabolism (LXR, PPAR, and cholesterol) and found significant upregulation of key target genes (Fig. 3A and B, Dataset S2) from the PPAR and/or cholesterol pathways and to a lower extent from LXR and LXR/cholesterol-overlapping pathways. To obtain a better understanding of the contribution of the individual histone deacetylases inhibited by MS-275, we used isogenic HAP1 cell lines with either complete knock-out of HDAC1, HDAC2 or HDAC3 or the corresponding knock-in mutants producing stable but catalytically inactive variants (HDAC1 H141A, HDAC2 H142A, and HDAC3 H135A) instead of the wild-type enzymes, resulting in the integration of non-functional HDACs into co-repressor complexes. The latter strategy was applied to prevent compensatory upregulation and integration of other HDACs into co-repressor complexes, thereby more closely mimicking the pharmacological inhibition with HDAC inhibitors (Moos et al., manuscript in preparation). The RT-qPCR analysis revealed that the lack of distinct class I HDACs results in upregulation of selected

key genes in macrophage lipid metabolism, like LXR-regulated cholesterol efflux transporters, *ABCA1* and *ABCG1* (Fig. 3C and D) and key players in lipid uptake and clearance (*CD36* and *FABP4)* linked to PPARγ pathways (Fig. 3E and F). However, this observed altered expression might be independent of changes in acetylation patterns at specific gene regions.

Intriguingly, when comparing the dosage effects of the pan-HDAC inhibitor SAHA and the class I-specific HDAC inhibitor MS-275 on the regulation of the same lipid metabolism-associated genes in human macrophages, we found that treatment with MS-275 showed a higher potency than SAHA for upregulating these genes (Fig. 4A–E). These results indicate that in human macrophages, especially class I HDACs play an important role in regulating lipid homeostasis and, thus, constitute a potential target for prevention of foam cell formation.

The class I-specific HDAC inhibitor MS-275 reduces human foam cell formation

Based on our findings that class I HDACs regulate genes associated with lipid metabolism in human macrophages, we analyzed the efficacy of MS-275 to improve lipid
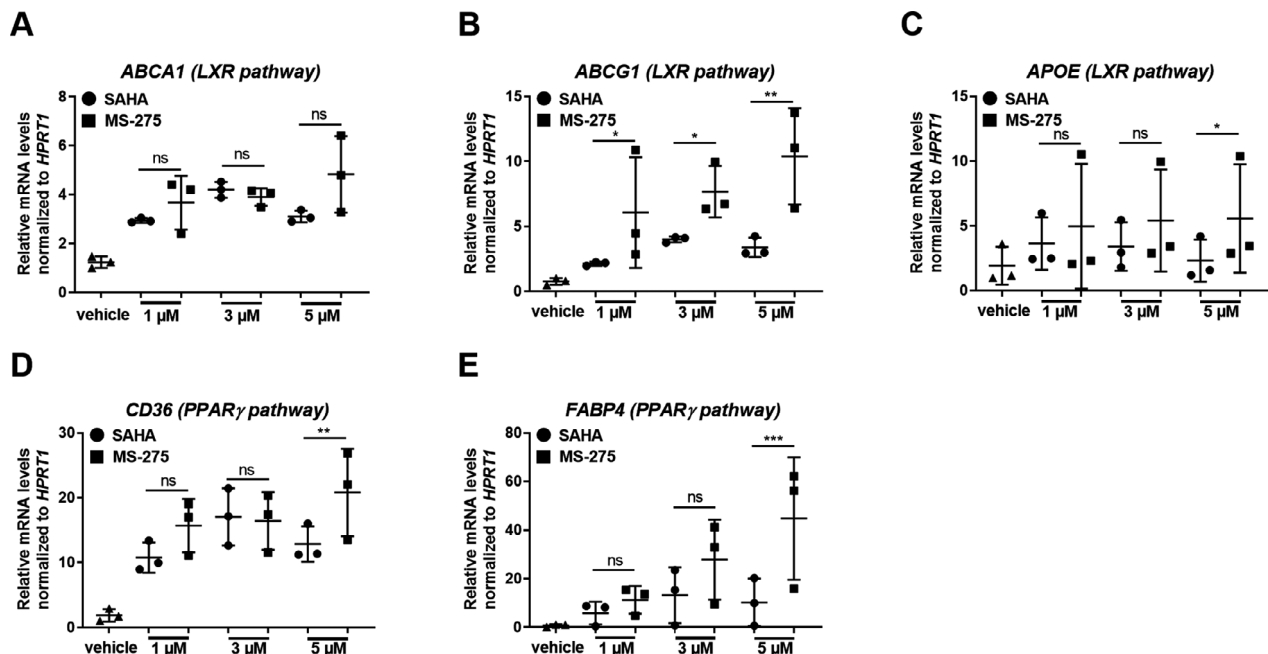

Figure 4. Inhibition of class I HDACs by MS-275 regulates lipid metabolism-associated genes in the human primary macrophages in vitro. (A–E) To determine the role of class I HDAC inhibition in human macrophages, CD14+ monocytes were isolated from the blood of three healthy controls and differentiated for 7 days using 50 ng/mL M-CSF. Mature M-CSF-dependent macrophages were incubated with different doses of MS-275 or the pan-HDAC inhibitor SAHA or vehicle (DMSO) control as indicated. After 24 h of incubation, expression levels of the LXR-regulated genes *ABCA1, ABCG1* and *APOE* (A–C) and the PPARγ-regulated genes *CD36* and *FABP4* (D and E) were measured by RT-qPCR and normalized to the reference gene *HPRT1*. The mean for each group is depicted and error bars indicate standard deviation. For statistical analysis, one-way ANOVA and Fisher's LSD test were used to compare samples treated with SAHA to MS-275-treated samples. *ns* = not significant, *$P < 0.05$, **$P < 0.01$, ***$P < 0.001$, ****$P < 0.0001$.

homeostasis using myelin-laden human macrophages. In vitro-differentiation in the presence of myelin debris for 7 days resulted in enlarged macrophages with foam-like morphology (Fig. 5A and C), as evidenced by ORO staining for neutral lipids including cholesterol esters. Without myelin exposure the macrophages showed an elongated morphology, typical for non-activated, anti-inflammatory cells in vitro, and only scarce lipid inclusions (Fig. 5B). Treatment of the lipid-laden macrophages with MS-275 (Fig. 5D and E) significantly reduced the number of foam cells and increased the frequency of cells with an elongated shape in comparison to vehicle-treated cells (Fig. 5F). Whereas myelin uptake elevated the amount of total cellular cholesterol (Fig. 5G), mainly containing free cholesterol, treatment with MS-275 significantly lowered the intracellular total cholesterol content of macrophages upon prolonged myelin loading. Interestingly, even the basal cholesterol levels of non-loaded macrophages could be downregulated with MS-275 (Fig. 5G). To further confirm that MS-275 interferes with lipid-enriched myelin accumulation, macrophages were incubated with pHrodo Green-labeled myelin and analyzed by flow cytometry. Here, we consistently found a significant reduction of pHrodo Green-positive foam cells indicating a possible increased net efflux of myelin-associated lipids/cholesterol upon 2-day-treatment with 2.5 μmol/L MS-275 (Fig. 5H).

Next, we assessed whether the observed lowered lipid accumulation in foam cells and, hence, possibly also tissue clearance, after MS-275 treatment is mediated by the induction of genes involved in lipid uptake and export. Indeed, RT-qPCR analysis revealed that MS-275 treatment resulted in a dose-dependent upregulation of *ABCG1, CD36, FABP4,* and *SOAT* (Fig. 6A–F). In addition, protein expression of the lipid exporters ABCA1 and ABCG1 and the scavenger receptor CD36 crucial for lipid uptake were further confirmed by flow cytometry analysis (Fig. S3).

Taken together, our findings indicate that inhibition of class I HDACs by MS-275 treatment leads to reduced lipid accumulation with concurrent upregulation of genes involved in cholesterol and fatty acid transport and adoption of an anti-inflammatory morphology in human foam cells generated in vitro.

MS-275 improves impaired lipid homeostasis and immune functions in macrophages from X-ALD patients

In the pathological context of X-ALD, we explored whether class I HDAC inhibition by MS-275 would improve the metabolic and immunological phenotype of *ABCD1*-deficient macrophages, which accumulate high levels of VLCFAs. Firstly, we found that the selective inhibition of class I HDAC members in HAP1 cells leads to a significant upregulation of the *ABCD2* gene (Fig. 7A), which upon overexpression can compensate for ABCD1 deficiency in X-ALD cells.[32–35] We recently found that pan-HDAC inhibition with Vorinostat (SAHA) stimulates *ABCD2* expression in human macrophages.[20] Interestingly, the class I-specific inhibitor, MS-275 not only caused a greater *ABCD2* induction when compared to SAHA (Fig. 7B) but also efficiently induced *ABCD2* expression at low doses (Fig. 7C). When analyzing the peroxisomal β-oxidation of the VLCFA C26:0, MS-275, and SAHA stimulated the rate of VLCFA degradation to a similar extent (Fig. 7D). A 5-day-treatment with 0.5 μmol/L MS-275 or 2.5 μmol/L SAHA significantly downregulated the accumulation of C26:0-lysophosphatidylcholine (C26:0-LPC) (Fig. 7E), albeit the levels were still higher than those observed in healthy control cells.

We have previously demonstrated that the disturbed lipid homeostasis in X-ALD macrophages results in pro-inflammatory skewing and impaired plasticity[8] and recently found that SAHA treatment partially rescued this phenotype.[20] Strikingly, MS-275-treatment almost completely abolished the IL12p40 secretion in LPS-stimulated X-ALD macrophages (Fig. 7F). Finally, we analyzed the effect of MS-275 on the ability of LPS-stimulated X-ALD macrophages to attract monocytes in a Boyden chamber. For this, we applied supernatants harvested from X-ALD macrophages, which had been LPS-activated in the presence of either MS-275 or vehicle. Although statistical significance was not reached, we found a trend for lower numbers of migrating monocytes with supernatants derived from pro-inflammatory X-ALD macrophages treated with MS-275 in comparison to vehicle control (Fig. 7G, $P = 0.057$).

Discussion

In CALD and MS, neuroinflammation is accompanied by the presence of enlarged foamy macrophages with increased intracellular lipid content and altered lipid homeostasis.[36,37] These foam cells are thought to contribute to maladaptive immune responses and, thus, may represent a novel target for pharmacologic interventions against the pathogenesis and progression of neuroinflammatory demyelinating diseases.[6] In active CALD lesions, we previously found a pronounced pro-inflammatory phenotype of foam cells as shown by enlarged macrophages with reduced expression of anti-inflammatory markers compared to MS.[8] Here, we found that especially enlarged foam cells coincided with a pro-inflammatory CD86-positive and active, phagocytic CD68-positive
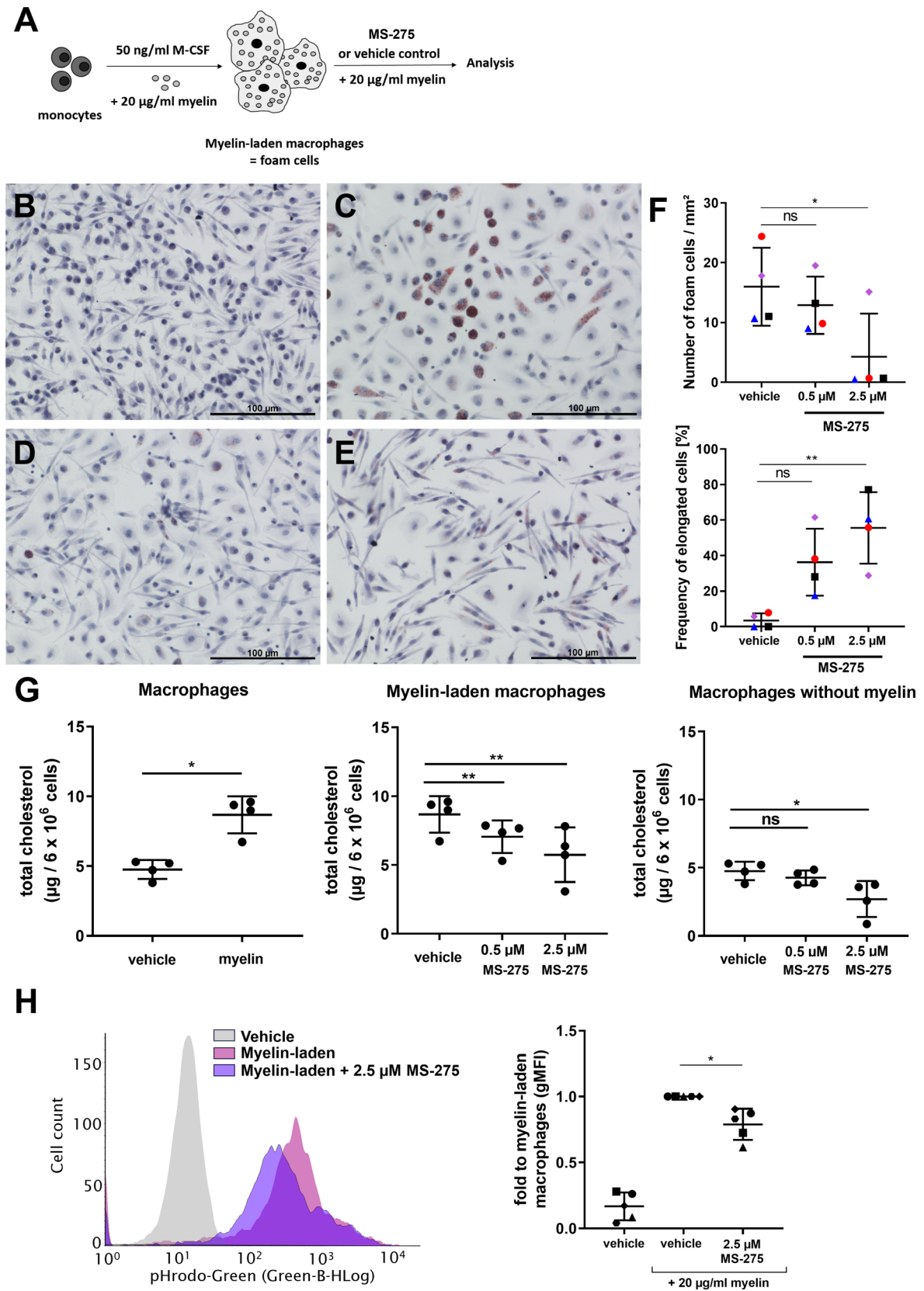
Figure 5. MS-275 treatment restores lipid homeostasis in myelin-laden foam cells in vitro. (A) Experimental strategy: Human foam cells were generated in vitro by differentiating monocyte-derived macrophages with M-CSF in the presence of 20 μg/mL myelin for 7 days. Foam cells were treated with MS-275 or vehicle (DMSO) control in the presence of myelin for 48 h before analysis. (B–F) Neutral lipids were stained by Oil Red-O in untreated macrophages without myelin (B), foam cells treated with vehicle control (C), foam cells treated with 0.5 μmol/L MS-275 (D) or 2.5 μmol/L MS-275 (E). Scale bar = 100 μm. (F) The number of foam cells and the frequency (%) of elongated-shaped macrophages (resembling normal morphology) were determined in samples derived from four healthy controls. (G) Macrophages without myelin or with myelin were treated with vehicle control, 0.5 μmol/L MS-275 or 2.5 μmol/L MS-275. After 48 h, the total cholesterol content (μg) was determined in cell lysates of 6×10^6 macrophages (pools of 3 wells per condition and proband) ($n = 4$). (H) Macrophages from five healthy controls were loaded with pHrodo-Green labeled myelin and treated as described in (A) before detachment for analysis by flow cytometry. The right panel depicts the geometric mean fluorescence intensity (gMFI) of MS-275-treated as fold-change to vehicle-treated myelin-laden macrophages derived from five healthy controls. For statistical analysis, one-way ANOVA and Fisher's LSD test was used when comparing vehicle control to MS-275 treatment. Two-tailed Student's *t* test was performed to analyze the difference of cholesterol between vehicle and myelin-treated macrophages in (G) and for analysis of absolute values used to generate the fold-change display in (H). ns = not significant, *$P < 0.05$, **$P < 0.01$.

phenotype. Immunometabolism studies have revealed that activation and function of macrophages are modulated by altered metabolic profiles.[38–40] With foam cells representing dysfunctional macrophages, pharmacological reprogramming of their lipid metabolism could be a novel therapeutic strategy. Because previous studies by others identified HDAC3 as a key regulator of lipid metabolism in murine macrophages,[21] we here analyzed the role of class I HDAC1-3 in human cells and the potential to improve lipid metabolism by their pharmacological inhibition using MS-275.

The whole-transcriptome analysis of human foamy macrophages from healthy donors indicated that myelin loading induced genes associated with lipid transport and efflux, whereas genes for fatty acid and cholesterol synthesis were found to be downregulated. Thus, healthy human macrophages apparently can effectively remove lipid-enriched myelin in vitro, possibly by inducing pathways
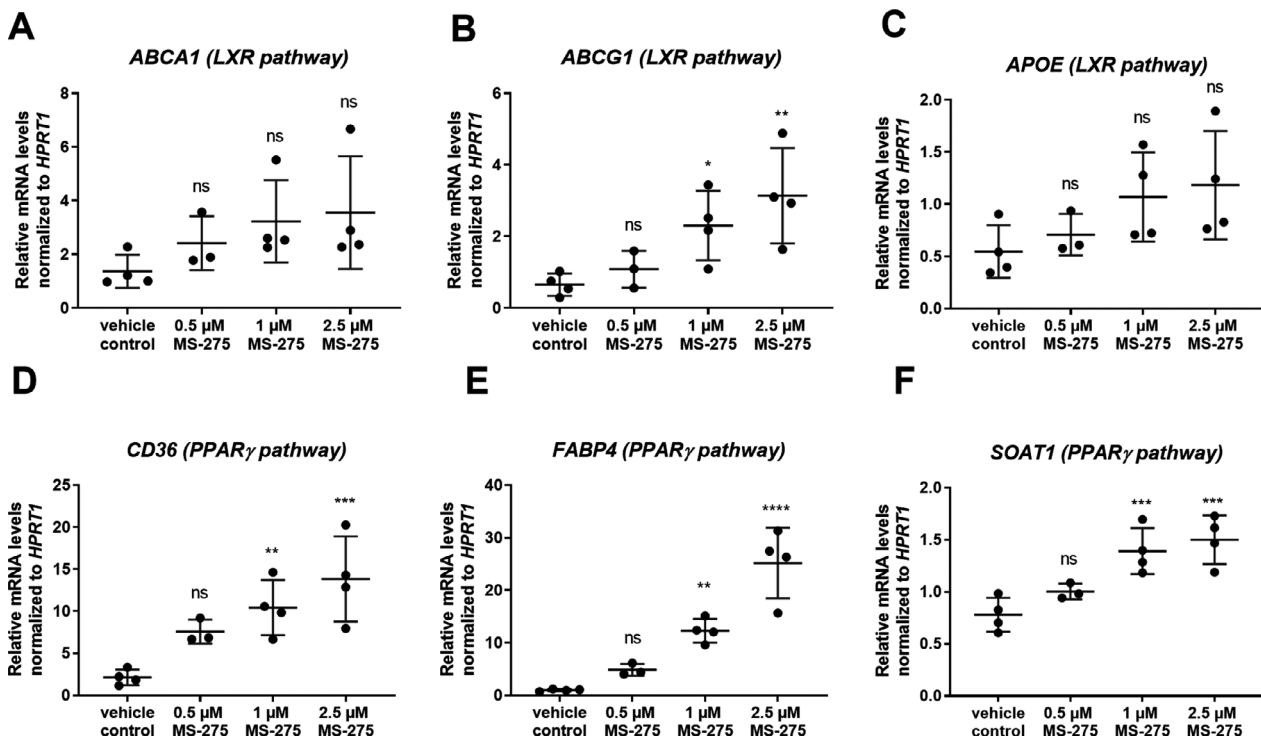

Figure 6. Pharmacological inhibition of class I HDACs by MS-275 leads to upregulation of lipid metabolism-associated genes in human foam cells. (A–F) To investigate the effect of MS-275 on foam cells, macrophages from four healthy donors were loaded with 20 μg/mL myelin during M-CSF-dependent differentiation for 7 days and then treated with vehicle control, 0.5, 1 or 2.5 μmol/L MS-275 in the presence of myelin for further 24 h. Relative expression of the indicated genes involved in lipid metabolism regulated by LXR (A–C) or PPARγ (D–F) were analyzed by RT-qPCR and normalized to mRNA levels of *HPRT1*. Mean and standard deviation are shown. For statistical analysis, one-way ANOVA and Fisher's LSD test were used. ns = not significant, *$P < 0.05$, **$P < 0.01$, ***$P < 0.001$, ****$P < 0.0001$.
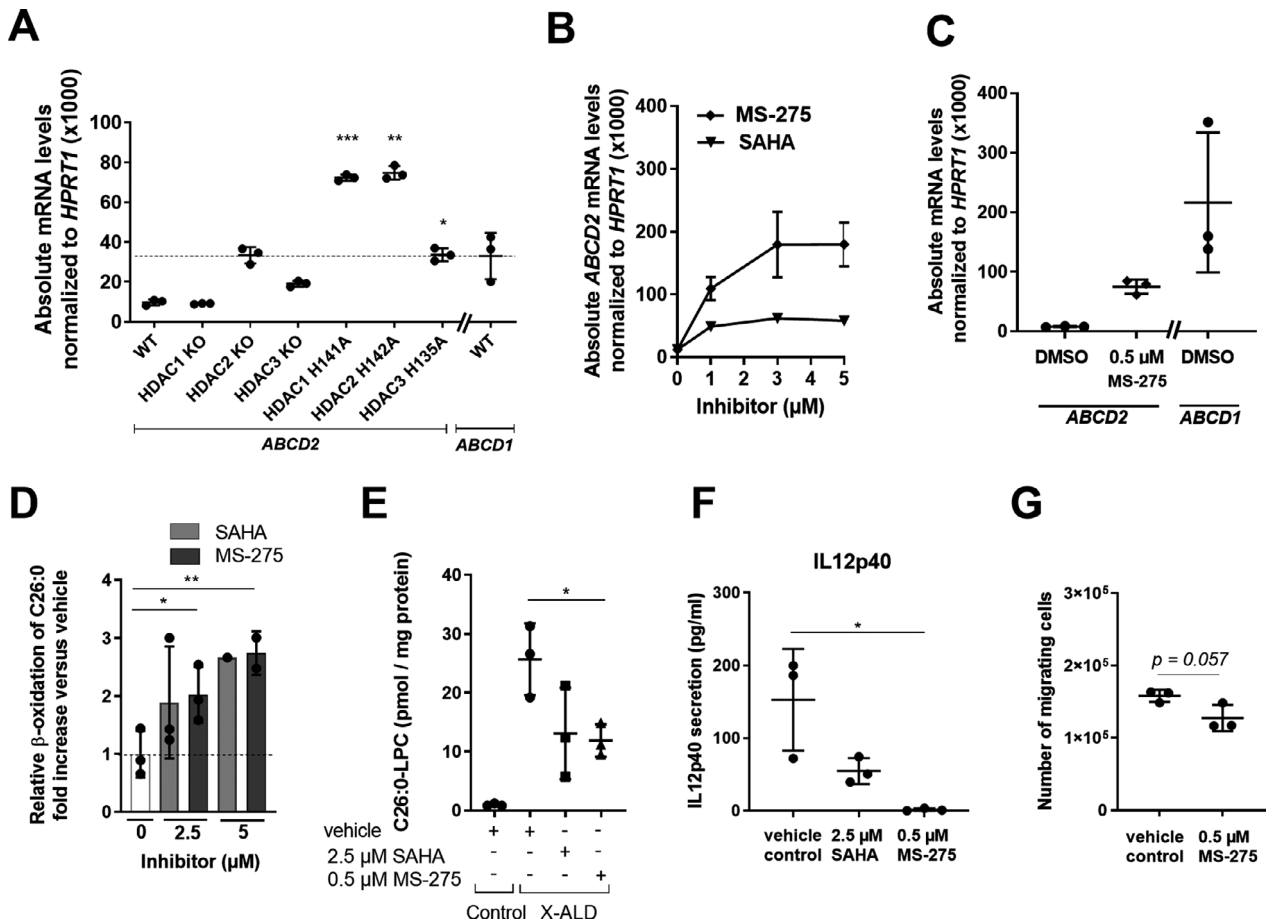
Figure 7. Inhibition of class I HDACs leads to *ABCD2* induction and improved metabolic and immunological dysfunction in human X-ALD macrophages. (A) Expression of the *ABCD2* gene was analyzed in wild-type (WT) or mutant HAP1 cells with either full knockout of HDAC1, 2 or 3 (KO) or isogenic lines expressing stable but enzymatically inactive proteins (HDAC1 H141A, HDAC 2 H142A or HDAC3 H135A). Absolute *ABCD2* and, for reference, *ABCD1* mRNA levels were analyzed and normalized to *HPRT1* using RT-qPCR. The dashed line marks the level of *ABCD1* mRNA in WT HAP1 cells. (B and C) Human macrophages (M-CSF-dependent) derived from three healthy donors were treated with vehicle control, SAHA or MS-275 for 24 h as indicated. *ABCD1* and *ABCD2* mRNA levels were analyzed as described for (A). (D) The degradation of the VLCFA C26:0 was determined in macrophages derived from three healthy controls that had been anti-inflammatory polarized with IL-4 and treated with vehicle control, SAHA or MS-275 for 48 h. The β-oxidation rates were normalized to protein content and are depicted as fold increase over the vehicle control. (E) The levels of C26:0-lysophophatidylcholin (LPC) were determined by LC–MS/MS after 5 days of treatment with vehicle or HDAC inhibitor (SAHA or MS-275). The results of macrophages derived from three healthy donors and three X-ALD patients are shown normalized to protein content. (F and G) Macrophages derived from three X-ALD patients were stimulated with LPS for 24 h in presence of either vehicle, 2.5 μmol/L SAHA or 0.5 μmol/L MS-275. The pro-inflammatory cytokine IL12p40 secreted into the supernatant was determined by ELISA (F). (G) These cytokine-containing supernatants from X-ALD macrophages were used in Boyden chambers to attract monocytes from a healthy donor. The number of migrating monocytes was determined after 12 h. Means and standard deviations are shown. For statistical analysis one-way ANOVA and Fisher's LSD test were used in (A) and (D) and two-tailed Student's *t*-test was performed in (E and F). In (A), statistical analysis was only applied for the HAP1 cells with enzymatically inactive HDACs compared to wild type (WT) HAP1 cells. *ns* = not significant, *$P < 0.05$, **$P < 0.01$, ***$P < 0.001$, ****$P < 0.0001$.

regulated by LXRα and PPARγ. When comparing genes from the cytokine/cytokine receptor pathway, mostly pro-inflammatory genes as defined by others[41] were downregulated, which is in good agreement with previous reports that myelin after proper degradation first initiates an anti-inflammatory program. Interestingly, the top 20 significantly upregulated genes are linked to cell differentiation,

proliferation and other homeostatic functions, which are also important for tissue regeneration. However, a clear anti-inflammatory signature was not indicated in these human foam cells in vitro. Instead, some of the upregulated genes (e.g., *CXCL8*) reflect a typical pro-inflammatory program. These results imply that upon sustained myelin phagocytosis, healthy human macrophages initiate

a metabolic program to support tissue regeneration but lack a distinct anti-inflammatory phenotype.

Whole-transcriptome analysis of MS-275-treated HAP1 cells revealed significantly upregulated genes involved in lipid metabolism, with pronounced induction of genes linked to LXR, PPARγ, and cholesterol. These pathways are known to be associated with lipid degradation and export but also with the induction of an anti-inflammatory program in immune cells.[6,27,42,43] Interestingly, a previous study found that in particular inhibiting the class I HDACs, however, independent of regulating the LXR pathway, upregulated the secretion of ApoE in a human astrocytoma cell line.[44] In the CNS, ApoE is an important protein required for the binding and the export of lipids. A schematic summary of MS-275-regulated lipid pathways in human HAP1 cells and primary macrophages is shown in Figure 8. Noteworthy, MS275-treated primary human microglia were not considered in our study and might behave differently. Specifically, we found MS-275-mediated induction of the genes for scavenger receptors CD36 and oxidized low-density lipoprotein receptor 1 (LOX-1, encoded by *OLR1*), and the fatty acid binding proteins long-chain fatty acid transport protein 6 (FATP 6, encoded by *SLC27A6*) and low-density lipoprotein receptor-related protein 2 (LRP2), which are crucial for lipid uptake and/or tissue clearance of apoptotic cells. This indicates that MS-275 would support clearance of myelin debris and apoptotic cells and, thus, possibly prevent or ameliorate persistent tissue inflammation. Following ingestion of myelin degradation products, the lipid-enriched debris and lipids are normally trafficked by endosomes/lysosomes and/or specific transporters to the endoplasmic reticulum (ER) for further breakdown, modification and esterification. Intriguingly, we found that MS-275 strongly upregulated *GRAMD1C* encoding the cholesterol transporter Aster-C (ASTRC) and to a lesser extent sterol O-acyltransferase 1 (SOAT1, alias ACAT1), an enzyme catalyzing the esterification of free cholesterol to cholesterol esters for further lipid sequestration. This indicates that inhibition of class I HDACs also would enhance the trafficking of phagocytosed lipids for further storage and/or sequestration and degradation. Upregulated expression of the ER-localized enzyme stearoyl-CoA desaturase 5 (SCD5), suggests that MS-275 may also promote the formation of anti-inflammatory, monounsaturated fatty acids. We additionally found increased mRNA levels for long-chain-fatty-acid-CoA ligase 3 (ACSL3), which, among other functions, mediates the fast and efficient relocation of lipids from the ER into lipid droplets for long-term storage, thus, preventing ER stress. In macrophages, lipid droplets are thought to be pseudo-organelles, which in addition to lipid storage also modulate immune responses by producing inflammatory mediators like eicosanoids.[7] Accordingly, by preventing formation of lipid droplets or promoting their degradation in macrophages, their activation status may be further reduced. Intriguingly, at the same time, MS-275 upregulated the expression of both genes encoding the key enzymes involved in breakdown of cholesterol esters and triglycerides in lipid droplets, lysosomal acid lipase/cholesteryl ester hydrolase (LAL, encoded by *LIPA*) and neutral cholesterol ester hydrolase 1 (NCEH1). Finally, class I HDAC inhibition resulted in stimulation of lipid export from the cells by inducing the ATP-binding cassette-transporters, ABCA1 and ABCG1, with the latter accounting for about 60% of the net lipid efflux in macrophages.[45–47]

Interestingly, *RXRG* was one of the most prominently upregulated genes in human HAP1 cells after treatment with MS-275. *RXRG* is only expressed at low levels in human monocytes and monocyte-derived macrophages. However, a previous study revealed that the corresponding protein isoform, RXRγ, is required for oligodendrocyte differentiation and appears to be a key factor during remyelination.[48] Previously, significant epigenetic changes were observed in oligodendrocytes in normal appearing white matter when analyzing postmortem brain tissue of CALD patients.[49] Therefore, treatment with MS-275 may exert positive effects on cell types other than macrophages in CNS lesions and might be subject to future studies.

The analysis of the role of individual members of the class I HDACs in the enzymatically inactive HDAC1, 2 or 3 mutant HAP1 cells revealed especially HDAC2 as a major regulator of LXR- and PPARγ-responsive genes involved in cholesterol and fatty acid homeostasis (e.g., *ABCG1, CD36,* and *FABP4*). These findings support the concept of a prominent role for class I HDACs in regulating lipid homeostasis in human cells.

In general, foam cell formation in CNS lesions has previously been associated with dysregulated cholesterol metabolism.[6] In a mouse model for focal demyelinating lesions induced by injections of lysolecithin, needle-like cholesterol crystals accumulating in macrophages were identified to inhibit expression of the lipid efflux transporters, ABCA1 and ABCG1, as well as the lipid acceptor ApoE.[1] When these mice were treated with the LXR agonist GW3965, the impaired gene expression was restored and an increased ability for remyelination and repair of CNS lesions was observed.[1] In CALD, active demyelinating lesions are especially enriched in cholesterol esters also containing VLCFA[50,51] and furthermore, needle-like structures have been observed in macrophages present in tissues with high cholesterol turnover in X-ALD patients.[36] Accordingly, upregulation of the LXR pathway by MS-275 treatment could possibly prevent cholesterol accumulation in macrophages and promote repair of CNS lesions. In X-ALD-derived macrophages, we found reduced pro-
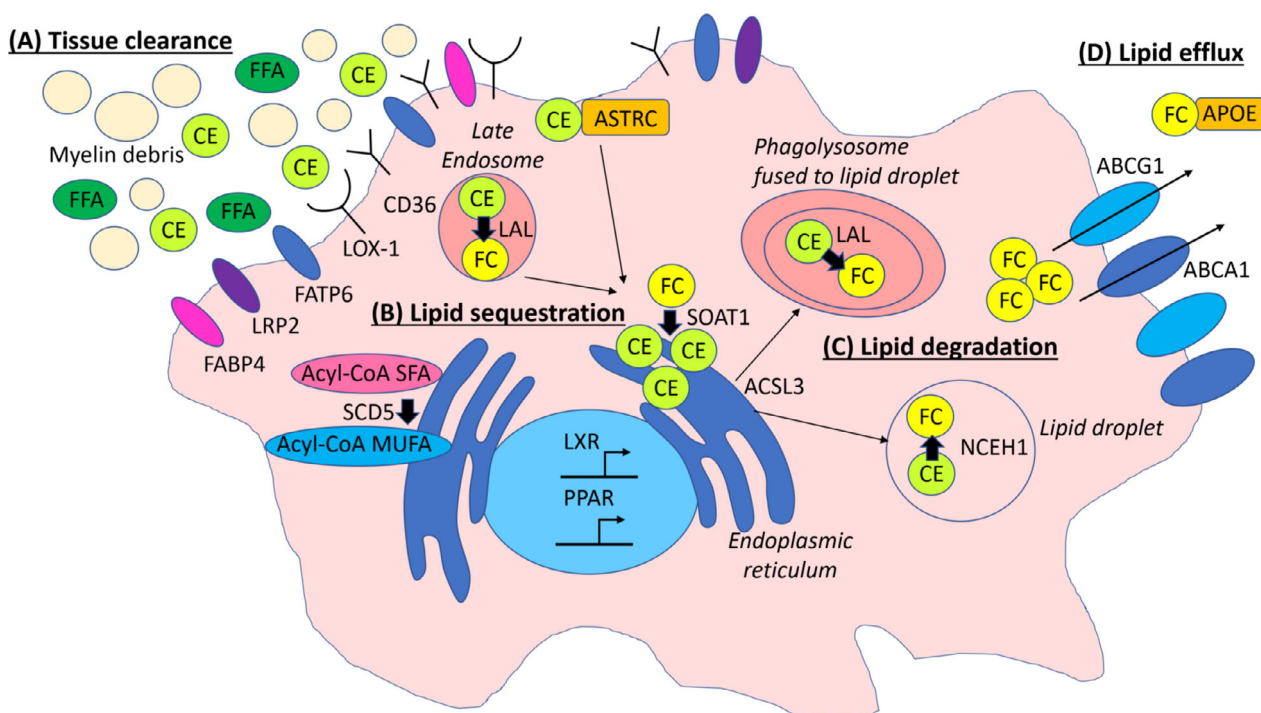
Figure 8. Hypothetical model explaining the metabolic reprogramming in human macrophages through inhibition of class I HDACs by MS-275. The treatment of human myelin-laden macrophages with MS-275 leads to upregulation of LXR and PPAR-regulated genes and reduces the number of pro-inflammatory foam cells in vitro. Based on our results, we hypothesize that MS-275 treatment could be beneficial in inflammatory demyelinating diseases by promoting (A) efficient tissue clearance of cell debris, (B) sequestration and storage of lipids and (C and D) hydrolysis of lipids for subsequent efflux. (A) The effective clearance of lipid-enriched myelin, including free fatty acids (FFA) and cholesterol ester (CE), and apoptotic cells from the microenvironment is a prerequisite for the establishment of an anti-inflammatory milieu in CNS lesions. This could be enabled by the MS-275-mediated upregulation of the receptors and fatty acid binding proteins CD36, LOX-1, FATP6, FABP4 and LRP2. After uptake by macrophages/microglial cells, lipids are shuttled to the endoplasmic reticulum (ER) either by the upregulated cholesterol transporter ASTRC in a non-vesicular manner or within the late endosome where CEs are enzymatically cleaved to free fatty acids and cholesterol (FC) by LAL. (B) At the ER, SOAT1 esterifies FC to CE for further storage. SCD5 catalyzes the desaturation of saturated fatty acyl-CoA (SFA), which generates anti-inflammatory, monounsaturated fatty acyl-CoA (MUFAs). To avoid ER stress, the fatty acyl-CoA synthetase ACSL3 promotes the formation of lipids droplets and, thus, the relocation of lipids within the cell. (C) The hydrolysis of CEs to free cholesterol occurs within lipid droplets by either NCEH1 or during lipophagy mediated by LAL within phagolysosomes. (D) Finally, free cholesterol can be exported by the cholesterol transporters ABCA1 and ABCG1. In the CNS, APOE binds free cholesterol for reverse cholesterol transport. CD36, Cluster of differentiation 36 molecule; LOX-1, Lectin-like oxidized LDL receptor 1; FATP6, Long-chain fatty acid transport protein 6; FABP4, Fatty acid-binding protein; LRP2, Low-density lipoprotein receptor-related protein 2; SOAT1, Sterol O-acyltransferase 1; APOE, Apolipoprotein E; ASTRC, Protein Aster-C; PPAR, Peroxisome proliferator-activated receptor; LXR, Liver X receptor; LAL, Lysosomal acid lipase/cholesteryl ester hydrolase; SCD5, Stearoyl-CoA desaturase 5; ACSL3, Long-chain-fatty-acid-CoA ligase 3.

inflammatory skewing as well as disease-associated accumulation of VLCFAs after MS-275 treatment, possibly due to the strongly induced expression of the redundant *ABCD2* gene, which has compensatory capacity in *ABCD1* deficiency.[32–35] The mechanism underlying *ABCD2* induction could either be directly related to histone acetylation at the *ABCD2* promoter, possibly involving a transcription factor complex of specificity protein 1/3 (Sp1/Sp3) associated with HDAC1.[52,53] Alternatively, because *ABCD2* is a cholesterol regulated gene, in turn activating the sterol regulatory element-binding proteins (SREBPs) known to bind and activate the *ABCD2* promoter,[52,54]

could cause induction of *ABCD2*. In addition, a previous study already suggested that the treatment with SAHA (Vorinostat), also inhibiting the class I HDAC family, has a positive effect on the disease progression in the experimental autoimmune encephalomyelitis (EAE) mouse model in vivo, a clinically important model for MS.[55] However, future studies are required to show possible beneficial effects of the specific class I HDAC inhibitor MS275 in EAE and MS, respectively.

We conclude that inhibition of class I HDACs by MS-275 treatment might not only enhance the uptake capacity for myelin debris by modulation of molecules crucial

for lipid uptake (e.g., CD36) but also concomitantly reduce foam cell formation of human macrophages. Such inhibitors can directly, at the level of gene expression, alter the lipid metabolism of macrophages and, therefore, enable the induction of an anti-inflammatory program, making class I HDAC inhibition in macrophages a promising novel target for inflammatory demyelinating diseases like CALD and MS.

Acknowledgments

Conflict of Interest

The authors declare no competing interests.

Author Contributions

B Zierfuss, I Weinhofer, C Seiser, and J Berger contributed to conceptualization. I Weinhofer, B Zierfuss, A Buda, N Popitsch, L Hess, V Moos, S Hametner, S Kemp, W Köhler, and C Seiser contributed to methodology. I Weinhofer, B Zierfuss, A Buda, N Popitsch, L Hess, V Moos, S Hametner, S Kemp, W Köhler, S Forss-Petter, and C Seiser contributed to investigations. B Zierfuss, I Weinhofer, S Forss-Petter, and J Berger contributed to writing. J Berger and C Seiser contributed to funding acquisition.

References

1. Cantuti-Castelvetri L, Fitzner D, Bosch-Queralt M, et al. Defective cholesterol clearance limits remyelination in the aged central nervous system. Science 2018;359:684–688.

2. Prinz M, Priller J. Microglia and brain macrophages in the molecular age: from origin to neuropsychiatric disease. Nat Rev Neurosci 2014;15:300–312.

3. Gitik M, Liraz-Zaltsman S, Oldenborg P-A, et al. Myelin down-regulates myelin phagocytosis by microglia and macrophages through interactions between CD47 on myelin and SIRPα (signal regulatory protein-α) on phagocytes. J Neuroinflammation 2011;8:24.

4. Kotter MR, Li W-W, Zhao C, Franklin RJM. Myelin impairs CNS remyelination by inhibiting oligodendrocyte precursor cell differentiation. J Neurosci 2006;26:328–332.

5. Boven LA, Van Meurs M, Van Zwam M, et al. Myelin-laden macrophages are anti-inflammatory, consistent with foam cells in multiple sclerosis. Brain 2006;129:517–526.

6. Grajchen E, Hendriks JJA, Bogie JFJ. The physiology of foamy phagocytes in multiple sclerosis. Acta Neuropathol Commun 2018;6:124.

7. Guerrini V, Gennaro ML. Foam cells: one size doesn't fit all. Trends Immunol 2019;40:1163–1179.

8. Weinhofer I, Zierfuss B, Hametner S, et al. Impaired plasticity of macrophages in X-linked adrenoleukodystrophy. Brain 2018;141:2329–2342.

9. Moser HW, Smith KD, Watkins PA, et al. X-linked adrenoleukodystrophy. In: A. L. Scriver Beaudet, W. S. Sly, D. C. R. Valle, eds. The metabolic and molecular bases of inherited disease. New York: McGraw Hill, 2001:3257–3301.

10. Mosser J, Douar AM, Sarde CO, et al. Putative X-linked adrenoleukodystrophy gene shares unexpected homology with ABC transporters. Nature 1993;361:726–730.

11. Wiesinger C, Kunze M, Regelsberger G, et al. Impaired very long-chain acyl-CoA beta-oxidation in human X-linked adrenoleukodystrophy fibroblasts is a direct consequence of ABCD1 transporter dysfunction. J Biol Chem 2013;288:19269–19279.

12. Berger J, Gartner J. X-linked adrenoleukodystrophy: clinical, biochemical and pathogenetic aspects. Biochim Biophys Acta 2006;1763:1721–1732.

13. Kemp S, Berger J, Aubourg P. X-linked adrenoleukodystrophy: clinical, metabolic, genetic and pathophysiological aspects. Biochim Biophys Acta (BBA)-Molecular Basis Dis 2012;1822:1465–1474.

14. Berger J, Forss-Petter S, Eichler FS. Pathophysiology of X-linked adrenoleukodystrophy. Biochimie 2014;98:135–142.

15. Kemp S, Huffnagel IC, Linthorst GE, et al. Adrenoleukodystrophy – neuroendocrine pathogenesis and redefinition of natural history. Nat Rev Endocrinol 2016;12:606–615.

16. Cartier N, Hacein-Bey-Abina S, Bartholomae CC, et al. Hematopoietic stem cell gene therapy with a lentiviral vector in X-linked adrenoleukodystrophy. Science 2009;326:818–823.

17. Eichler F, Duncan C, Musolino PL, et al. Hematopoietic stem-cell gene therapy for cerebral adrenoleukodystrophy. N Engl J Med 2017;377:1630–1638.

18. Raymond GV, Aubourg P, Paker A, et al. Survival and functional outcomes in boys with cerebral adrenoleukodystrophy with and without hematopoietic stem cell transplantation. Biol Blood Marrow Transplant 2019;25:538–548.

19. Weber FD, Wiesinger C, Forss-Petter S, et al. X-linked adrenoleukodystrophy: very long-chain fatty acid metabolism is severely impaired in monocytes but not in lymphocytes. Hum Mol Genet 2014;23:2542–2550.

20. Zierfuss B, Weinhofer I, Kühl J-S, et al. Vorinostat in the acute neuroinflammatory form of X-linked adrenoleukodystrophy. Ann Clin Transl Neurol 2020;7:639–652.

21. Hoeksema MA, Gijbels MJ, Van den Bossche J, et al. Targeting macrophage Histone deacetylase 3 stabilizes atherosclerotic lesions. EMBO Mol Med 2014;6:1124–1132.

22. Van Den Bossche J, Neele AE, Hoeksema MA, et al. Inhibiting epigenetic enzymes to improve atherogenic macrophage functions. Biochem Biophys Res Commun 2014;455:396–402.

23. Van Den Bossche J, Neele AE, Hoeksema MA, De Winther MPJ. Macrophage polarization: the epigenetic point of view. Curr Opin Lipidol 2014;25:367–373.

24. Huffnagel IC, van de Beek M-C, Showers AL, et al. Comparison of C26:0-carnitine and C26:0-lysophosphatidylcholine as diagnostic markers in dried blood spots from newborns and patients with adrenoleukodystrophy. Mol Genet Metab 2017;122:209–215.

25. Frischer JM, Bramow S, Dal-Bianco A, et al. The relation between inflammation and neurodegeneration in multiple sclerosis brains. Brain 2009;132(Pt 5):1175–1189.

26. Bogie JFJ, Timmermans S, Huynh-Thu VA, et al. Myelin-derived lipids modulate macrophage activity by liver X receptor activation. PLoS One 2012;7:e44998.

27. Bogie JFJ, Jorissen W, Mailleux J, et al. Myelin alters the inflammatory phenotype of macrophages by activating PPARs. Acta Neuropathol Commun 2014;2:43.

28. Natrajan MS, Komori M, Kosa P, et al. Pioglitazone regulates myelin phagocytosis and multiple sclerosis monocytes. Ann Clin Transl Neurol 2015;2:1071–1084.

29. Kroner A, Greenhalgh AD, Zarruk JG, et al. TNF and increased intracellular iron alter macrophage polarization to a detrimental M1 phenotype in the injured spinal cord. Neuron 2014;83:1098–1116.

30. Mailleux J, Vanmierlo T, Bogie JFJ, et al. Active liver X receptor signaling in phagocytes in multiple sclerosis lesions. Mult Scler J 2018;24:279–289.

31. Carette JE, Raaben M, Wong AC, et al. Ebola virus entry requires the cholesterol transporter Niemann-Pick C1. Nature 2011;477:340–343.

32. Netik A, Forss-Petter S, Holzinger A, et al. Adrenoleukodystrophy-related protein can compensate functionally for adrenoleukodystrophy protein deficiency (X-ALD): implications for therapy. Hum Mol Genet 1999;8:907–913.

33. Kemp S, Wei H-M, Lu J-F, et al. Gene redundancy and pharmacological gene therapy: implications for X-linked adrenoleukodystrophy. Nat Med 1998;4:1261–1268.

34. Muneer Z, Wiesinger C, Voigtländer T, et al. Abcd2 is a strong modifier of the metabolic impairments in peritoneal macrophages of ABCD1-deficient mice. PLoS One 2014;9:e108655.

35. Pujol A, Ferrer I, Camps C, et al. Functional overlap between ABCD1 (ALD) and ABCD2 (ALDR) transporters: a therapeutic target for X-adrenoleukodystrophy. Hum Mol Genet 2004;13:2997–3006.

36. Schaumburg HH, Powers JM, Suzuki K, Raine CS. Adreno-leukodystrophy (sex-linked Schilder disease): ultrastructural demonstration of specific cytoplasmic inclusions in the central nervous system. Arch Neurol 1974;31:210–213.

37. Schaumburg HH, Powers JM, Raine CS, et al. Adrenoleukodystrophy. A clinical and pathological study of 17 cases. Arch Neurol 1975;32:577–591.

38. Zhu L, Zhao Q, Yang T, et al. Cellular metabolism and macrophage functional polarization. Int Rev Immunol 2015;34:82–100.

39. Wynn TA, Chawla A, Pollard JW. Macrophage biology in development, homeostasis and disease. Nature 2013;496:445–455.

40. Koo S-J, Garg NJ. Metabolic programming of macrophage functions and pathogens control. Redox Biol 2019;24:101198.

41. Mantovani A, Sica A, Sozzani S, et al. The chemokine system in diverse forms of macrophage activation and polarization. Trends Immunol 2004;25:677–686.

42. Martin H. Role of PPAR-gamma in inflammation. Prospects for therapeutic intervention by food components. Mutat Res - Fundam Mol Mech Mutagen 2010;690:57–63.

43. Pascual G, Fong AL, Ogawa S, et al. A SUMOylation-dependent pathway mediates transrepression of inflammatory response genes by PPAR-γ. Nature 2005;437:759–763.

44. Dresselhaus E, Duerr JM, Vincent F, et al. Class I HDAC inhibition is a novel pathway for regulating astrocytic apoE secretion. PLoS One 2018;13:e0194661.

45. Jakobsson T, Venteclef N, Toresson G, et al. GPS2 Is required for cholesterol efflux by triggering histone demethylation, LXR recruitment, and coregulator assembly at the ABCG1 locus. Mol Cell 2009;34:510–518.

46. Kennedy MA, Barrera GC, Nakamura K, et al. ABCG1 has a critical role in mediating cholesterol efflux to HDL and preventing cellular lipid accumulation. Cell Metab 2005;1:121–131.

47. Wang X, Collins HL, Ranalletta M, et al. Macrophage ABCA1 and ABCG1, but not SR-BI, promote macrophage reverse cholesterol transport in vivo. J Clin Invest 2007;117:2216–2224.

48. Huang JK, Jarjour AA, Nait Oumesmar B, et al. Retinoid X receptor gamma signaling accelerates CNS remyelination. Nat Neurosci 2010;14:45–53.

49. Schlüter A, Sandoval J, Fourcade S, et al. Epigenomic signature of adrenoleukodystrophy predicts compromised oligodendrocyte differentiation. Brain Pathol 2018;28:902–919.

50. Igarashi M, Schaumburg HH, Powers J, et al. Fatty acid abnormality in adrenoleukodystrophy. J Neurochem 1976;26:851–860.

51. Theda C, Moser AB, Powers JM, Moser HW. Phospholipids in X-linked adrenoleukodystrophy white

matter: fatty acid abnormalities before the onset of demyelination. J Neurol Sci 1992;110:195–204.

52. Weinhofer I, Forss-Petter S, Žigman M, Berger J. Cholesterol regulates ABCD2 expression: implications for the therapy of X-linked adrenoleukodystrophy. Hum Mol Genet 2002;11:2701–2708.

53. Doetzlhofer A, Rotheneder H, Lagger G, et al. Histone deacetylase 1 can repress transcription by binding to Sp1. Mol Cell Biol 1999;19:5504–5511.

54. Weinhofer I, Kunze M, Rampler H, et al. Liver X receptor alpha interferes with SREBP1c-mediated Abcd2 expression. Novel cross-talk in gene regulation. J Biol Chem 2005;280:41243–41251.

55. Ge Z, Da Y, Xue Z, et al. Vorinostat, a histone deacetylase inhibitor, suppresses dendritic cell function and ameliorates experimental autoimmune encephalomyelitis. Exp Neurol 2013;241:56–66.

Supporting Information

Additional supporting information may be found online in the Supporting Information section at the end of the article.

Figure S1. Principal component analysis (PCA) of human macrophages without and with myelin exposure.
Figure S2. Cell size determination of foam cells within CNS lesions using two different staining procedures.
Figure S3. Flow cytometry analysis of MS-275-treated human myelin-laden macrophages.
Table S1. Description of controls and X-ALD patients.
Table S2. Demographics and clinical characteristics of the CALD and MS cases.
Table S3. Primers and probes.
Supplementary Materials & Methods.

Flow cytometry analysis of MS-275-treated foam cells
Assessment of cytokine secretion by ELISA
Human monocyte migration assay
Peroxisomal β-oxidation of 1-^{14}C-labeled fatty acids
Lipid analysis

Dataset S1. Targeted analysis of genes from cholesterol, LXR, or PPAR pathways and cytokine-cytokine receptor interaction pathway in human myelin-laden macrophages.
Dataset S2. Significantly changed genes from the cholesterol, LXR, or PPAR pathways in MS-275-treated HAP-1 cells.